JOURNAL OF AIRCRAFT
Vol. 35, No. 3, May–June 1998

Effects of Fin and Jet Vortex Generators on the Crossflow

Todd G. Wetzel* and Roger L. Simpson†
Virginia Polytechnic Institute and State University, Blacksburg, Virginia 24061

The effect of fin and jet vortex generators on the crossflow separation of a submersible vehicle in a sideslip was studied. The sideslip orientation simulates the dominant features of a turning maneuver. The vortex generators are located on the top and bottom centerline of the body to improve turning performance by changing the crossflow separation and the resultant hydrodynamic forces. Oil-flow visualization and force and moment measurements are used as the primary diagnostics. The fins are found to be very effective in delaying crossflow separation, while the jets were not. In addition, the oil flows revealed the importance of locating vortex generators near the bow and the critical role a forward-mounted, low-aspect-ratio appendage plays in the near-body fluid dynamics. Overall the fins were found to be viable as a concept for flow control, while the jets employed were not. The concept of using vortex generators to control flow separation and thus forces and moments applies equally well to all bodies of revolution, including aircraft fuselages and missiles.

Nomenclature

C_l = roll moment coefficient, body axes, L/qc^3
C_m = pitching moment coefficient, about $x/c = 0.29$, body axes, M/qc^3
C_n = yaw moment coefficient, about $x/c = 0.29$, body axes, N/qc^3
C_x = axial force coefficient, body axes, X/qc^2
C_y = normal or side force coefficient, body axes, Y/qc^2
C_z = vertical force coefficient, body axes, Z/qc^2
c = submersible vehicle chord (length)
D_f = distance between fins
h = height of fins
L = roll moment, body axes
M = pitching moment, body axes
N = yaw moment, body axes
n = number of vortex generators
p = freestream pressure
p_0 = fan chamber pressure
q = dynamic pressure, $(1/2)\rho U_\infty^2$
R = gas constant
Re = chord Reynolds number, $\rho U_\infty c/\mu$
Re_θ = momentum thickness Reynolds number, $\rho U_\infty \theta/\mu$
R_1 = primary reattachment
R_2 = secondary reattachment
S_{ref} = reference area
S_1 = primary separation
S_2 = secondary separation
T_j = fan chamber temperature
U_∞ = free-stream velocity
V_j = jet velocity
VR = velocity ratio, V_j/U_∞
X = axial force, body axes
x = longitudinal distance along submersible vehicle from nose
Y = normal or side force, body axes
Z = vertical force, body axes
β = sideslip angle
δ = boundary-layer thickness
δ^* = displacement thickness
θ = skew angle, referenced to model centerline; and momentum thickness
κ = linear jet speed/pressure slope
ρ = fluid density
ϕ = angular location around cross section measured from windward side
ϕ_i = inclination angle of jet to local surface

Introduction

TURNING maneuvers of submersible vehicles result in crossflow separation that generates large hydrodynamic forces and moments that negatively affect maneuverability.[1] Pearcey[2] and Bragg and Gregorek[3] showed that strategically placed vortex generators can be used to control two-dimensional flow separation on wings at stall. It is presumed that vortex generators can be used to control the three-dimensional crossflow separation on submersible vehicles in turning maneuvers.

Two concepts are pursued here. The first concept (Fig. 1a) calls for deployable fins as vortex generators that are free to move in both the amount of penetration into the flow and in the angle of skew to the local flow. The vortex generators should be deployable because the added drag of deployed vortex generators greatly detracts from cruise performance and stealth. The variable orientation allows adaptation to any particular flow situation encountered. The second concept (Fig. 1b) involves jets with variable strength and orientation. In either case the vortex generators are placed along the top and bottom centerlines of the submersible vehicle from bow to stern to energize the crossflow of the boundary layer and move the crossflow separation further around the leeside of the vehicle for either port or starboard turns. In actual implementation the orientation and penetration of the vortex generator system would be dependent on the instantaneous separation flow condition experienced by the vehicle.

Previous Research

Axisymmetric bodies yawed to the freestream flow, like submersible vehicles in a turning maneuver, produce large

Received March 3, 1997; revision received Dec. 16, 1997; accepted for publication Dec. 17, 1997.

*Research Associate, Department of Aerospace and Ocean Engineering; currently Heat Transfer Engineer, General Electric Corporate R&D Center. Member AIAA.

†Jack E. Cowling Professor, Department of Aerospace and Ocean Engineering. Fellow AIAA.

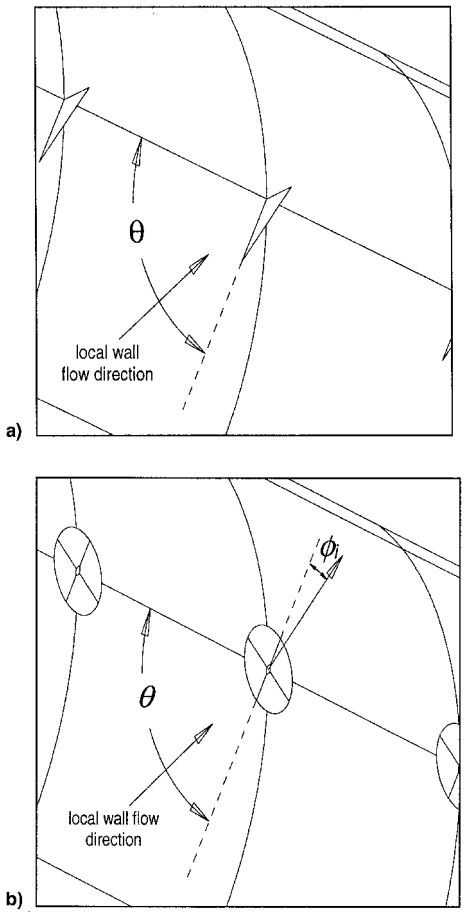

Fig. 1 a) Fin and b) jet configurations.

amounts of vortical separation. That vortical flow adversely affects acoustic and nonacoustic stealth, propulsion efficiency and body drag, control effectiveness, and maneuverability.[1] Figure 2 shows typical flow structures in such a crossflow separation.[4] For circular cylindrical bodies at 15-deg sideslip, the crossflow usually separates near $\phi = 105$ deg.[5]

These flows are highly sensitive to Reynolds number effects.[1] Ahn and Simpson[6] studied the vortical flow on a prolate spheroid at angle of attack. In such a case the primary separation location is largely dependent on the state of the boundary layer (laminar, transitional, or turbulent), which is a function of a Reynolds number. For high Reynolds number flows or flows with boundary-layer transition fixed such that the boundary layer is turbulent at separation, Ahn and Simpson show that the separation-line dependency on the Reynolds number is greatly reduced. The separation line no longer changes much circumferentially, but gradually extends upstream on the body with an increase in Reynolds number. At increasing angle of attack the separation line moves farther windward and farther upstream on the body.[1]

It is desirable to be able to control this flow separation. One device commonly used to reduce two-dimensional separation is the vortex generator. As viscous friction and adverse pressure gradients slow the boundary layer, separation becomes imminent.[2] The role of the vortex created by a vortex generator is to provide a mechanism whereby higher energy fluid outside the boundary layer can mix with the near-surface, low-velocity fluid to reenergize the boundary layer and delay or prevent separation. This idea can be extended to the more complex, three-dimensional vortical separation experienced by a yawed submersible vehicle.

While fins have been studied in detail their high drag has prompted researchers to look more closely at jets. Compton and Johnston[7] concluded that the three-dimensional flow structure of a jet vortex is similar to weak vortices generated by a solid vortex generator, but is different from the strong vortices of a large solid generator.

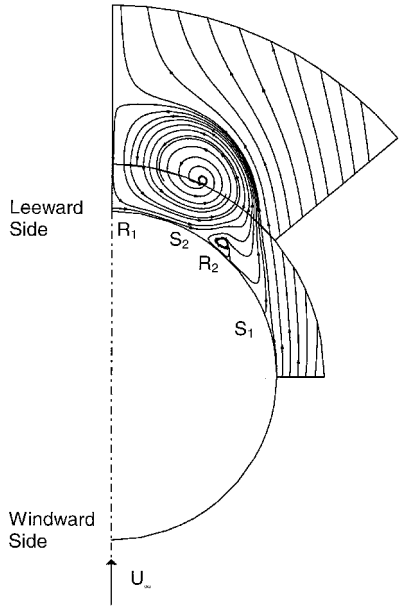

Fig. 2 Crossflow separation[4]: this half-cross-section of the submersible vehicle shows the important flow phenomena; the addition of vortex generators delays separation (*S*1 and *S*2) farther around the leeward side of the submersible vehicle.

Morin et al.[8,9] performed several experiments involving vortex generators in three-dimensional separation. In Ref. 9, vortex generators were used on a cylinder at very high angles of attack (50 and 70 deg) to successfully delay separation. In Ref. 8 vortex jets were used on a backward-facing curved ramp. The researchers reported that the jets did delay separation, but the results were far less dramatic than the solid generators in Ref. 9.

Bushnell and Donaldson[1] identify several potential problems for these configurations, including additional drag as a result of the fins or high-energy consumption for the jets, constantly changing flow conditions, and control system complication. With these problems in mind, Bushnell and Donaldson recommend that a successful vortex generator system would need to be "active, dispersed, rapidly deployable, and triggered by distributed sensors."

Vortex Generators: Types and Configurations

Half-delta wing vortex generators consist of small plates mounted normal to the local body surface and at incidence to the local near-wall flow (Fig. 1a). Other types of solid vortex generators include ramps, wedges, notches, fences, and riblets.[2] Pneumatic vortex generators include blowing and suction slots and jets. Most of the applications studied thus far have involved the control of vortex lift of high-performance aircraft.[10–13]

Different configurations of the vortex generators will offer various vortical structures and, therefore, various advantages and disadvantages. Corotating vortex generators produce several vortices that rotate in the same direction. Corotating systems offer relative insensitivity to spacing and local flow direction, and the vortical structure is relatively constant in the streamwise direction. These facts make the corotating vortex generators easiest to implement successfully. Also, because the flow separation off the submersible vehicle is vortical in nature, a unidirectional vortex is most suitable to counteract that separation. Other vortex generator systems include counterrotating and biplane vortex generators.[2]

Design and Considerations from Previous Work

Fins

The most important consideration in designing a vortex generator system is not the boundary-layer profile just upstream of the vortex generator but rather the range and severity of separation that needs to be controlled.[2] Corotating vortex generators will dampen the effects of one another if spaced too closely, and so Pearcey[2] suggests $D_f/h > 3$. Pearcey also notes that once above that minimum, vortex generator effectiveness drops off very slowly, so that values of D_f/h are often around 5 or 6.

Pearcey also stresses the importance of vortex generator uniformity. Nonuniform vortex generators create nonuniform vortices, which can result in "displacement of the vortices normal to the surface and relative to each other."[2]

Another important factor is the local angle of attack, or skew, of the fin. While in two-dimensional studies the freestream direction is constant and known, in three-dimensional flows the freestream direction can vary and is more difficult to predict with certainty. Therefore, skew angle θ in these studies is referenced from the model centerline and not from any local flow phenomenon.

The fins are almost always low-aspect-ratio rectangular plates, but more streamlined shapes can help alleviate drag penalties while retaining the original vortical effectiveness. Pearcey points out that the general goal in optimizing fin shape is to increase the lift-to-drag ratio of the fin, which results in the most vorticity for the least amount of drag. Airfoil shapes and camber may make vortex generators more efficient, but usually the scale involved in the tests is too small to account for such differences. Half-delta-wing vortex generators were found to have the least drag penalty in Bragg and Gregorek's[3] laminar-flow canard experiment.

Jets

Vortex jets are streams of fluid that flow from a nozzle in the surface at some skew angle to the freestream flow θ, and some inclination to the surface ϕ_i (Fig. 1b). As with the fins, θ is measured relative to the model centerline. The jet introduces velocity components normal to the freestream resulting in the vortex formation. Pearcey argues that a system of jets pointing in the same direction is analogous to a corotating system of solid vortex generators and, thus, suggests identical spacing criteria.

Several studies have focused attention on the inclination and skew angles. Lin et al.[14] studied two-dimensional separation and found the best inclination angle ϕ_i is between 15 and 25 deg and the best skew angle θ is between 60 and 120 deg. Morin et al.[9] used jets to control a three-dimensional separation and found optimal skew angles θ between 30 and 90 deg, but found no difference between inclination angles ϕ_i of 45 and 30 deg. The data of Ref. 9 also suggest that the jets are relatively ineffective.

The relative strength of the fluid jet is described by VR. As expected, jet effectiveness is proportional to VR, where effectiveness refers to the ability of the jet to change the flowfield, whether that change be the movement of a vortex or a separation line.[7,9,11,14,15]

Experimental Apparatus

Wind Tunnel

All of the tests were performed in the Virginia Polytechnic Institute and State University Stability Wind Tunnel. This continuous, closed-return, subsonic wind tunnel has a 7.6 m long, 1.8 × 1.8 m square interchangeable test section. The tunnel has a flow speed range of 0–70 m/s and a maximum unit Reynolds number of 5×10^5/m. The tunnel is powered by a 450-kW dc motor that turns a 4.25-m-diam prop. The flow is directed through screens and a 9:1 contraction and has a very low-turbulence intensity of less than 0.05%. The tunnel allows force and moment measurements to be taken from either a strut or sting-mounted strain gauge balance. The sting was selected for its lower interference with the flow.

Wind-Tunnel Models

Two submersible vehicle models were built from kits and detailed dimensions are given in Ref. 16. The models are 229 cm long and have a 21.0 cm maximum diameter. The model structures consist of a fiberglass skin mated to an aluminum skeleton. No propulsor or rear control surfaces were modeled. A longitudinal ridge and a forward-mounted appendage with fins were all modeled. The blackbody surface was marked with a white grid spaced every 10.2 cm in the longitudinal direction and every 45 deg in the circumferential direction. When the model was in the tunnel, all mounting holes were filled with red vacuum wax or plaster.

To trip the flow, circular posts 0.5 mm high, 2.54 mm center-to-center, and 1.3 mm in diameter were placed around the nose at $x/c = 0.044$ and along the length of the model at ± 45 deg from the windward side of the model. The trip strips were placed on the nose to guarantee tripped boundary layers at low angles of sideslip, while the longitudinal trips were effective for higher angles of sideslip. Trips were also placed on all appendages. Tests on model 1 indicated little Re dependence from $Re = 4.6 \times 10^6$ to 8.8×10^6, and so the trip strips were effective.[16]

To simulate a turning maneuver, the model was placed in a sideslip. The model was mounted in the tunnel on its side to utilize the adjustable angle-of-attack feature of the strut-mounted sting (Fig. 3). The longitudinal ridge was placed on the windward side so that a left turn was modeled. Sideslip angles of up to 15 deg were simulated.

Vortex Generators

It is difficult to transform Pearcey's sizing and spacing guidelines for vortex generators in two-dimensional flow to a three-dimensional problem.[2] The researchers arbitrarily selected the height and spacing of the fins, guaranteeing only that the height was more than the expected maximum boundary-layer thickness and the spacing ratio D_f/h was greater than 3. The jet spacing dimensionally matched the fin spacing. In all configurations the vortex generators were spaced 10.2 cm apart. The fin and jet configurations for each model are shown in Fig. 4.

Half-delta wings were used for the fins. The fins were made of sheet aluminum, were 25.4 mm long, 12.7 mm high, and 1.6 mm thick, and had leading and trailing edges that were rounded with a radius half the thickness of the fin. The fins were either glued directly to the model skin or attached to flush-mounted, rotatable disks embedded in the model body.

For the jets the air intake consists of two 3.2 × 203 mm slots located at peripheral angles of 90 and 270 deg and spanning from $x/c = 0.09$ to 0.18. Fine mesh screen was installed in the slots to make the intake flow more uniform over its area.

Fig. 3 Model in the wind tunnel.

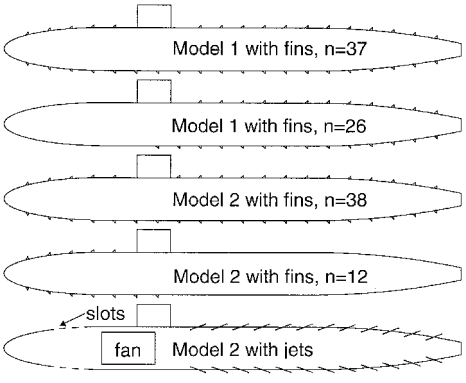

Fig. 4 Model fin and jet configurations; *n* is the number of fins.

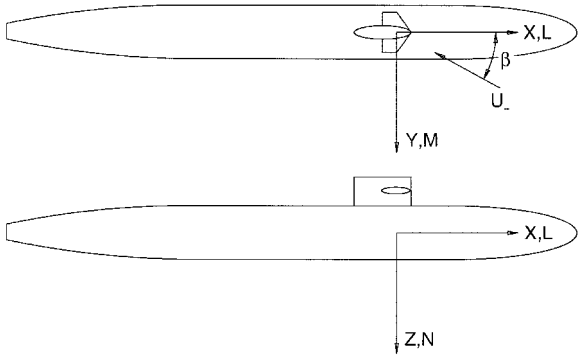

Fig. 5 Body-axes notation; moments taken about *x/c* = 0.29.

A Sears model 113.177460 wet/dry shop vac motor was mounted near the bow. The fan provides up to 16-kPa pressure at a flow rate of 300 L/min. The fan exhaust was distributed via a 2.5-cm-i.d. plastic tubing manifold, to 3-mm-i.d. plastic tubing, through a tapered 3 mm i.d. brass fitting, and finally to 24 jets, each 1.65-mm i.d. at 30-deg inclination. The total system could provide jets speeds of over 90 m/s. Jets were spaced every 10.2 cm from behind the forward-mounted appendage.

Instrumentation and Experimental Techniques

Forces and Moments

A six-component strain-gauge balance made by the Transducer Systems Division of Modern Machine and Tool, Inc., of Newport News, Virginia, was used for the force and moment measurements. All data were collected with a Hewlett-Packard model 3052 data acquisition unit. Each reading was the average of 50 values. The data are reported in body axes with the moments taken about the quarter chord of the forward-mounted appendage (Fig. 5), which is located at $x/c = 0.29$. Runs were made for wind-tunnel speeds of 30–60 m/s (Reynolds numbers of 4.60×10^6 to 8.77×10^6) and at sideslip angles of 0–15 deg. The uncertainties were estimated at 20:1 odds to be $\delta C_x = \pm 0.0001$, $\delta C_y = \pm 0.0002$, $\delta C_z = \pm 0.0002$, $\delta C_l = \pm 0.00002$, $\delta C_m = \pm 0.00005$, and $\delta C_n = \pm 0.0001$. All force and moment plots show the relative size of these uncertainties.

Oil Flows

A primary diagnostic for these tests was surface oil-flow visualization. Lines of separation are indicated by converging surface skin friction line patterns. The peripheral angle separation location ϕ is measured from the windward side, counterclockwise facing the model (Fig. 2). For a more detailed description of oil-flow visualization and its interpretation refer to Ref. 16.

Boundary-Layer Measurements

Hot-wire anemometer measurements were made to get an approximate boundary-layer thickness at the location of the vortex generators. A custom hot-wire rake with 16 logarithmically spaced gold-plated sensors over a 2.5-cm span was used to measure the u component of velocity simultaneously throughout the boundary layer. The rake was positioned as close to the body as possible at $x/c = 0.43$ and $\phi = 90$ deg. A detailed description of the probe, hot-wire electronics, and data acquisition are found in Ref. 17. A description of the calibration and application in this experiment can be found in Ref. 16.

Vortex Jets Data Acquisition

The pressure and temperature inside the fan canister were used to calculate the jet speed. The pressure was measured with a National Semiconductors LX1601A pressure transducer that was calibrated against the wind-tunnel's dynamic pressure transducer. The temperature was measured with an Omega type-k thermocouple and TAC80 thermocouple-to-analog converter.

To compute the jet velocity a relation that accounts for friction and expansion losses was developed that is represented by the form

$$V_j = \kappa\sqrt{RT_j[(p_o/p) - 1]}$$

which gives much more realistic results for the jet speed than does an isentropic relation. This equation was calibrated with a rotameter to determine the constant κ. The derivation for this relation can be found in Ref. 16. Jet speed uncertainties are $\pm -10\%$.

Experimental Results

Boundary-Layer Measurements

Boundary-layer profiles were taken at 0- to 15-deg sideslip and $Re = 4.6 \times 10^6$ and at 15-deg sideslip for $Re = 4.6 \times 10^6$ to 9.7×10. (The results are listed in Table 1). It is important to note that at the boundary-layer thickness at 15-deg sideslip and $Re = 6.8 \times 10^6$, the most common test case is 7.6 mm. This verifies that the 12.7-mm-high fins are scaled properly to the boundary-layer thickness.

Oil Flows

Model Without Vortex Generators

Fig. 6 shows the bottom of the submersible vehicle from $x/c = 0.576$ to 0.665 from the nose. This run was made at $\beta = 15$ deg and $Re = 6.78 \times 10^6$. Primary separation occurred at 97 deg on the forward-mounted appendage side and 115 deg on the bottom side of the submersible vehicle. Secondary lines of separation were also found in some of the cases.

Also, as shown in Fig. 7, the forward-mounted appendage plays a very important role in the flow development on the submersible vehicle. At $\beta = 15$ deg (Fig. 7), a large vortex sheds off the forward-mounted appendage. This is accompanied by a smaller vortex on the forward-mounted appendage itself, and a stagnation point/saddle point combination on the submersible vehicle behind the forward-mounted appendage. Because of the forward-mounted appendage appreciable dissimilarities between the forward-mounted appendage side and the bottom of the submersible vehicle should be expected.

Model with Fins

Fig. 8 shows the separation line for the same portion of the submersible vehicle as shown in Fig. 6 and at the same conditions ($\beta = 15$ deg, $Re = 6.78 \times 10^6$), but including the vortex-generating fins. The separation line has moved toward the leeside as compared to Fig. 6. Separation was delayed by as much as 33 deg on the appendage side and 37 deg on the bottom side. Local vortical wakes are evident for each vortex generator. In general, the oil-flow streaks are oriented more in a circumferential direction in this case compared to the case

Table 1 Boundary layer data at $x/c = 0.43$, $\phi = 90$ deg for different Re and β

Flow parameter					
Re	β, deg	δ, mm	δ^*, mm	θ, mm	Re_θ
4.92	0	12.7	2.57	1.90	3961
4.92	5	13.4	2.18	1.55	3523
4.91	10	10.6	1.51	1.09	2566
5.07	15	9.04	1.29	0.97	2657
7.36	15	6.99	0.87	0.64	2316
9.70	15	5.49	0.76	0.55	2363

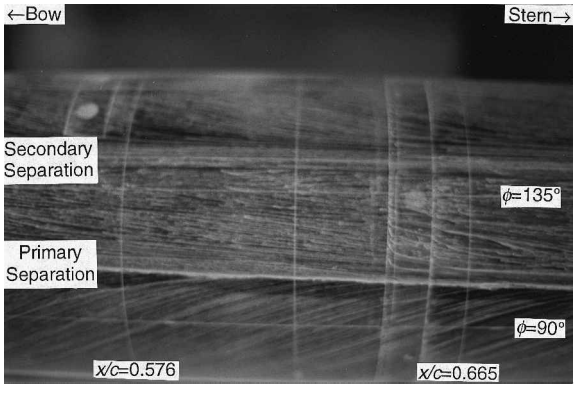

Fig. 6 Oil flow, naked submersible vehicle, $\beta = 15$ deg and $Re = 6.8 \times 10^6$. Left peripheral grid line is $x/c = 0.576$, right grid line is $x/c = 0.665$. The lower visible horizontal grid line is $\phi = 90$ deg, the higher grid line is $\phi = 135$ deg. Bottom of vehicle: note converging oil-flow lines around primary separation at $\phi = 115$ deg.

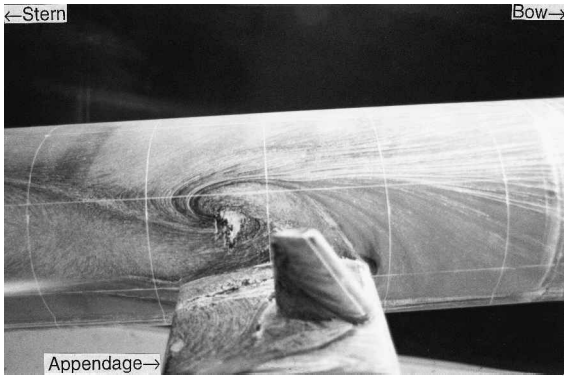

Fig. 7 Oil flow of vortical separation on leeside of appendage region; naked submersible vehicle, $\beta = 15$ deg and $Re = 6.8 \times 10^6$. Note trip posts near leading edges of appendage fins.

with no vortex generators. Also, the primary separation line, now at $\phi = 140$ deg compared to 115 deg without vortex generators, is wavy, varying by a few degrees circumferentially. The separation line is most leeward in the vicinity of the generator wakes and most windward between consecutive wakes.

Several observations were made during these runs. First, it is important to introduce vorticity relatively far upstream. In the initial vortex generator configuration, the first half-delta wing was placed at $x/c = 0.27$, delaying separation by almost 25 deg. Later configurations added vortex generators all the way from $x/c = 0.044$, with a subsequent additional delay in separation of 12 deg.

Model with Jets

To maximize the jet-velocity ratio VR at 3.54, the jets were tested at the lowest Reynolds number, $Re = 4.6 \times 10^6$. In this configuration, with $\phi_i = 30$ deg and $\theta = 90$ deg, there is no measurable improvement compared to the submersible vehicle

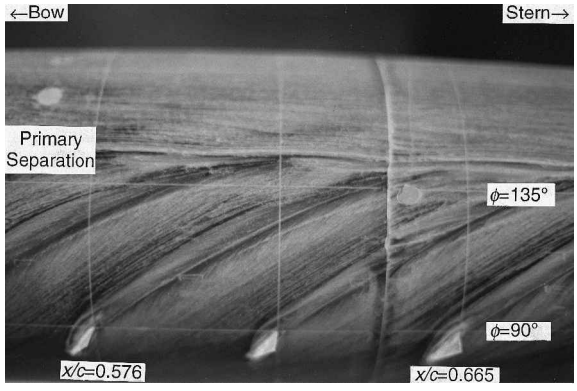

Fig. 8 Oil flow, submersible vehicle with fins, $\beta = 15$ deg and $Re = 6.4 \times 10^6$. Left grid line is $x/c = 0.576$, right grid line is $x/c = 0.665$. The lower visible horizontal grid line (where vortex generators are located) is $\phi = 90$ deg, while the higher grid line is $\phi = 135$ deg. Bottom of vehicle: primary separation is seen at $\phi = 152$ deg.

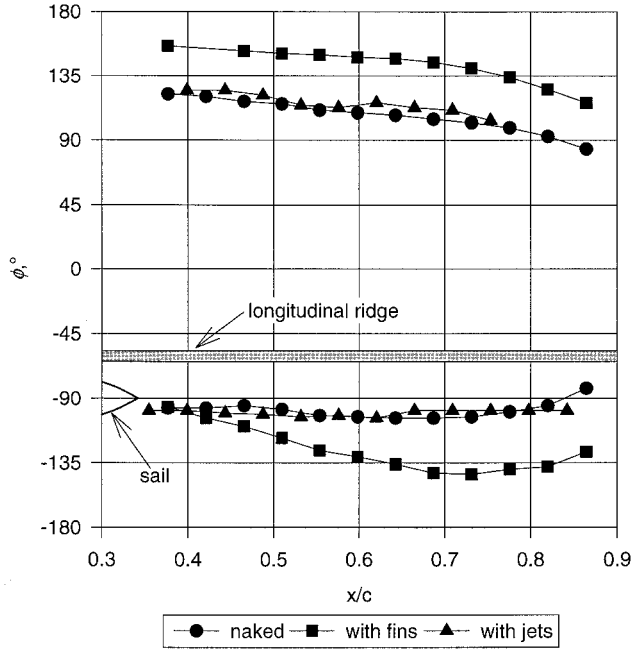

Fig. 9 Separation lines for the naked submersible vehicle and the submersible vehicle with fins and jets at $\beta = 15$ deg. Notice the large effect because of the fins. The shaded bar represents the location of the longitudinal ridge.

without jets (see Fig. 9). Therefore, the oil flows indicate that the jets are not effective. Possible reasons for jet ineffectiveness are discussed in the Forces and Moment Jets section later in this paper.

Force and Moment Fins

Figure 10 shows the variation of the force and moment coefficients with respect to sideslip β for both the model without generators (naked) and the model with vortex generating fins at different θ. The axial force does not vary much with increasing sideslip, but the separation off the body results in an increasingly negative side force and yaw moment. It is important to distinguish between the axial force, which in this case does not increase substantially with the angle of sideslip, and the drag, which is a trigonometric combination of the axial and side forces and is substantially increasing with sideslip angle. The increasing incidence of the forward-mounted appendage with increasing sideslip yields an increasingly negative roll moment. The fact that the normal force becomes increasingly positive and the pitch moment becomes increasingly

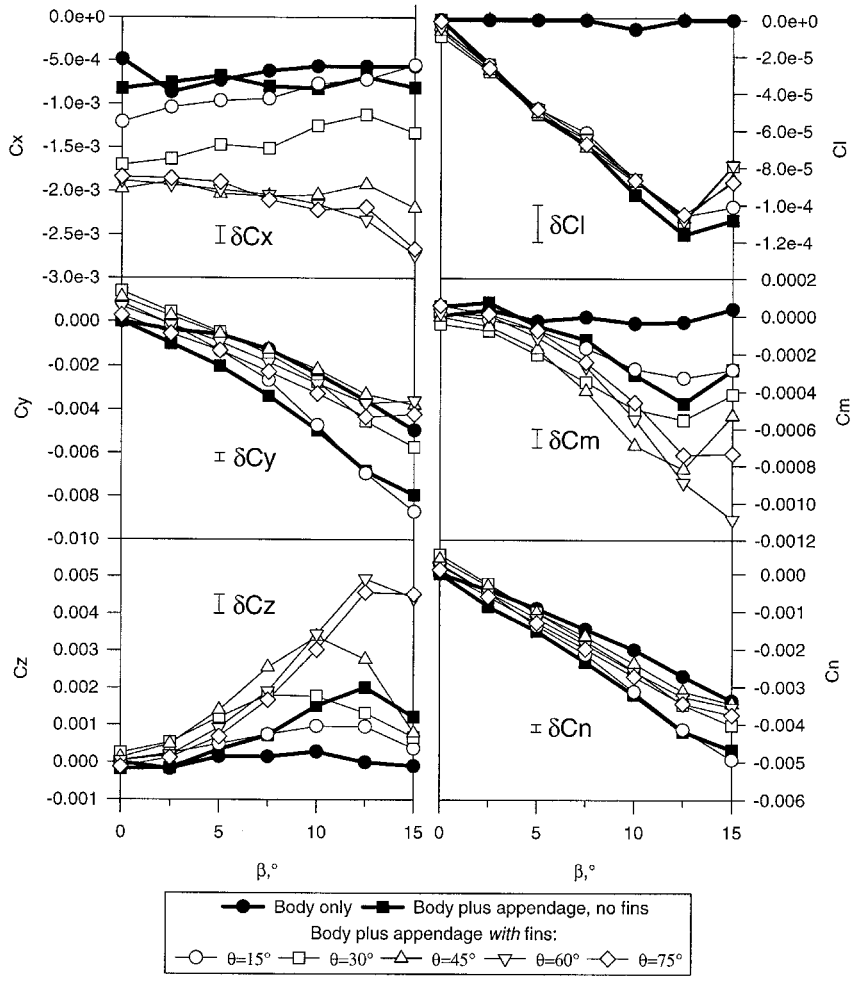

Fig. 10 Forces and moments vs sideslip for different θ for model 2 with 38 fins. $Re = 6.8 \times 10^6$.

negative is an artifact of the interaction between the appendage wake and the body separation.

The fins drastically change the forces and moments. The fins carry a huge drag penalty as C_x is doubled and sometimes tripled in the worst case. On the other hand, both the C_y and C_n experience a decrease in magnitude and, more importantly, a decrease in curve slope. C_y decreases by as much as 50%, whereas C_n decreases by as much as 35%.

The out-of-plane forces and moments are affected by the fins as well. C_l is unchanged, but both C_m and C_z increase by several orders of magnitude with the addition of the fins. These changes in the out-of-plane forces and moments are particularly important to measure because neither the sign nor the magnitude changes are intuitively predictable as a result of the highly nonlinear separation phenomena.[18] In fact, the vertical force becomes as large or larger than the side force and the axial force at some skew angles. The generation of a vertical force is a result of the interaction of the separation off the forward-mounted appendage with the separation off the body.

It is important to know whether the changes in the forces and moments by the fins are because of the additional forces and moments acting on each fin or because of resultant separation delay. Polhamus' method was used to estimate the forces acting on the fins.[19] Despite the fact that the fins are mostly submerged in the boundary layer, the approach velocity distribution was conservatively approximated as uniform, free-stream velocity. At β = 15 deg and θ = 55 deg, it was found that about 25% of C_x is caused by the fins directly, whereas the contribution to C_y was about 1% and the contribution to C_n was about 5%. Therefore, the changes in the forces and moments are principally a result of the delay in separation and not the forces acting on the individual fins themselves.

Only 25% of the change in axial force is a result of the fins directly. One might expect that delaying separation would decrease the drag on a body, and this is qualitatively true. This statement is not necessarily true for the axial force, however. If one transforms the force and moment data into a wind-axis system (lift and drag instead of axial force and normal force), one finds the fins account for 100% of the increase in body drag and essentially no increase in body lift.

Effect of Skew Angle

Figure 11 shows the change in forces and moments with fins plotted against skew angle θ for different β. For example, the $\Delta C_{()}$ change in axial force coefficient is

$$\Delta C_x(\beta) = C_x(\theta, \beta)\big|_{\text{with fins}} - C_x(\beta)\big|_{\text{no fins}}$$

The axial force plot shows that the drag penalty is worst at high skew angles. This penalty is finite and peaks out at about θ = 45 deg for the lower sideslip angles, or θ = 60 deg for higher sideslip. ΔCy and ΔCn both peak out at typically 45 deg skew. Although the C_l is unaffected, C_m and particularly C_z vary significantly with skew angle.

Effect of Number of Fins

A series of tests was run on each model to determine the variation of the forces and moments with the number of vortex generators at β = 15 deg, θ = 55 deg, and $Re = 6.8 \times 10^6$. These series began with all of the vortex generators on the

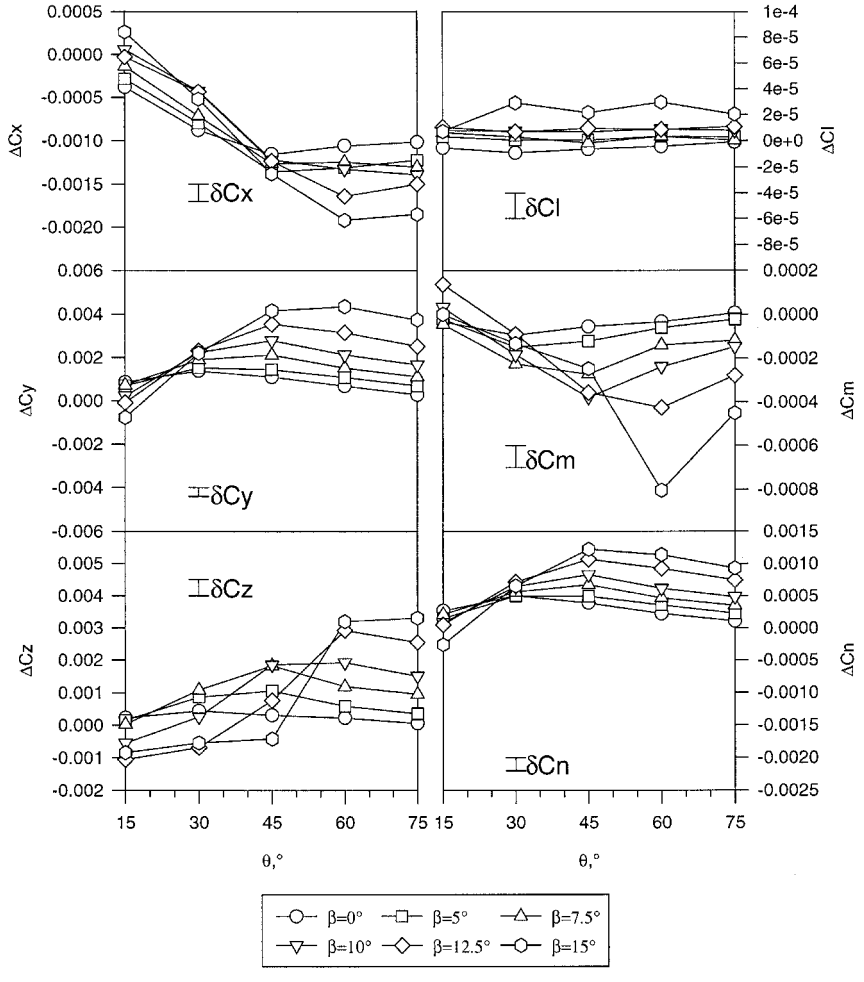

Fig. 11 Forces and moments vs θ (skew referenced from model centerline, Fig. 1) for model 2 with 38 fins. $Re = 6.8 \times 10^6$.

submersible vehicle. For each run, a pair of fins (one on the top, one on the bottom) was removed and forces and moments were measured. Series 1 involved removing the fins from the nose rearward, while series 2 involved removing the fins from the rear forward. Figure 4 shows comparative examples for each model with partial fin configurations. Note that model 2 does have one additional fin immediately downstream of the forward-mounted appendage that is not present on model 1. This series of tests essentially measured the effect of starting or ending location of the fin system on the forces and moments. It is important to note that there were several rows at the forward-mounted appendage where only one vortex generator was removed per run.

The results of these series are presented in Fig. 12. The presence of the forward-mounted appendage relative to the fin system plays an important role in the force and moment trends. For series 1 the forward-mounted appendage is at the front of the vortex generating system for $n = 26$ fins, whereas for series 2 the forward-mounted appendage is behind the fin system for $n = 12$. Also, the forces and moments do not exactly match up in the full vortex generator cases. The discrepancy is partially a result of uncertainties and differences between the two models (including the extra fin on model 2).

C_x varies linearly with the number of fins in both cases, which suggests that the drag is proportional to the number of fins. Using linear regression, the average contribution per fin to the axial force C_x was found to be 6.3×10^{-5}, or 6% of the baseline axial force. The normal force C_y varies somewhat linearly with an inflection point in both series at the forward-mounted appendage region. This indicates that the fins forward of the appendage do not play as important a role in the normal force as those aft of this appendage. C_n follows a similar trend,

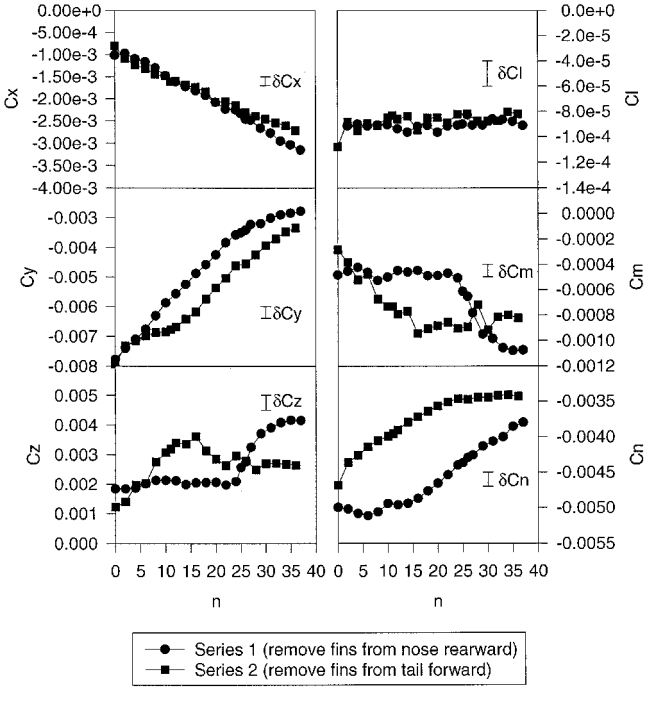

Fig. 12 Forces and moments vs number of vortex fins. β = 15 deg, θ = 55 deg, and $Re = 6.8 \times 10^6$. Series 1 involved removing fins from the nose rearward, while series 2 involved removing fins from the tail forward. Series 1 utilized model 1 while series 2 utilized model 2.

but this time it is the rear 10 or 15 fins that do not contribute much to the change in yaw moment.

The out-of-plane forces and moments (C_z, C_l, and C_m) follow interesting trends as well. As before, the roll moment is unchanged with or without fins. There is a huge inflection in the pitching moment and vertical force for series 1 in the forward-mounted appendage region. A similar trend is more subtle in series 2.

All of these inflection points in the forward-mounted appendage region are because of the fact that the presence of the forward-mounted appendage forces the separation line just aft of this appendage down to the appendage trailing edge regardless of the fin configuration employed. Therefore, the effectiveness of the fins on the top of the submersible vehicle in the vicinity of the forward-mounted appendage is less than that of the same fins on the bottom of the submersible vehicle or the fins on the top far aft of the forward-mounted appendage. The presence of the forward-mounted appendage results in a complex interaction between the appendage separation, the body separation, and the vortex generators, and as a result generates significant and peculiar off-axis forces and moments.

Force and Moment Jets

The jets were much less effective in changing the forces and moments. Figure 13 shows the variation of each of the forces and moments with β for VR = 3.54 and for all skew angles. The changes because of the jets are typically less than the uncertainties. It was conjectured that perhaps the jets were less effective because they weren't positioned far enough toward the bow. However, Fig. 12 shows the forces and moments for the fins in the exact configuration as the jets, corresponding to n = 24 of series 1 on the graphs. It is evident that the fins affect the forces and moments more drastically than those produced by a comparable jet configuration, even at high jet velocity ratios. The effect of the suction inlets on the nose in the present study is unknown but is assumed to be small.

The lack of jet effectiveness contradicts the positive results reported in Refs. 8, 14, and 15. Important flow parameters that define this flow include the strength of the adverse pressure gradient, the amount of surface curvature, Reynolds number, velocity ratio, and jet geometry. The conditions of Refs. 8, 14, and 15 span the conditions represented in the present work, although not all in the same combination. However, the present experiment is the only one that is fully three dimensional. Reference 8 is the only case that is not fully two dimensional. However, in Ref. 8 the flowfield is two dimensional upstream of the jets and 40 or more jet diameters downstream of the jets, suggesting that the vortex may be able to form completely within a two-dimensional boundary layer and persist into the three-dimensional separated region. It is possible that the skewing of a true three-dimensional boundary layer may adversely affect or even prevent the formation of a vortex by the jet. Of course, a solid generator in any nonparallel flowfield must create a vortex and therefore will be effective in either two- or three-dimensional flows.

Effect of Skew Angle

Figure 14 shows the variation of the forces and moments with skew angle for VR = 3.54 and various sideslip angles. The forces and moments show no significant variation with θ for the jet configuration used.

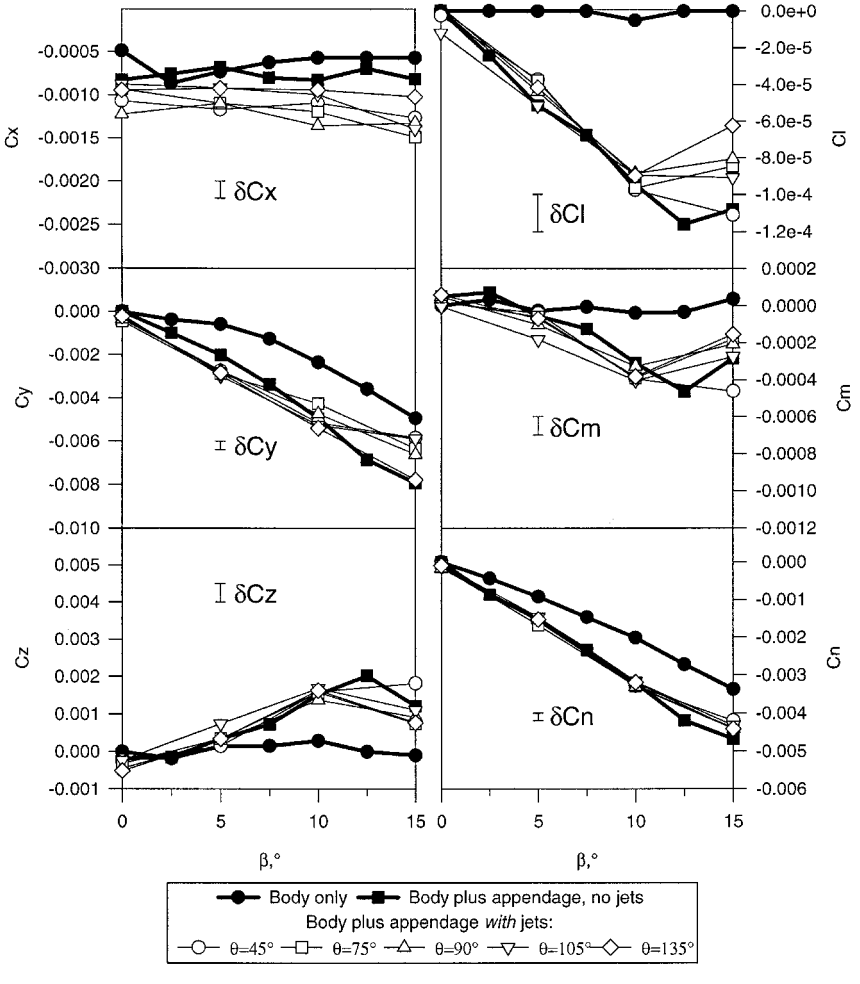

Fig. 13 Forces and moments vs sideslip for different θ for model 2 with jets. VR = 3 and Re = 4.6 × 10^6.

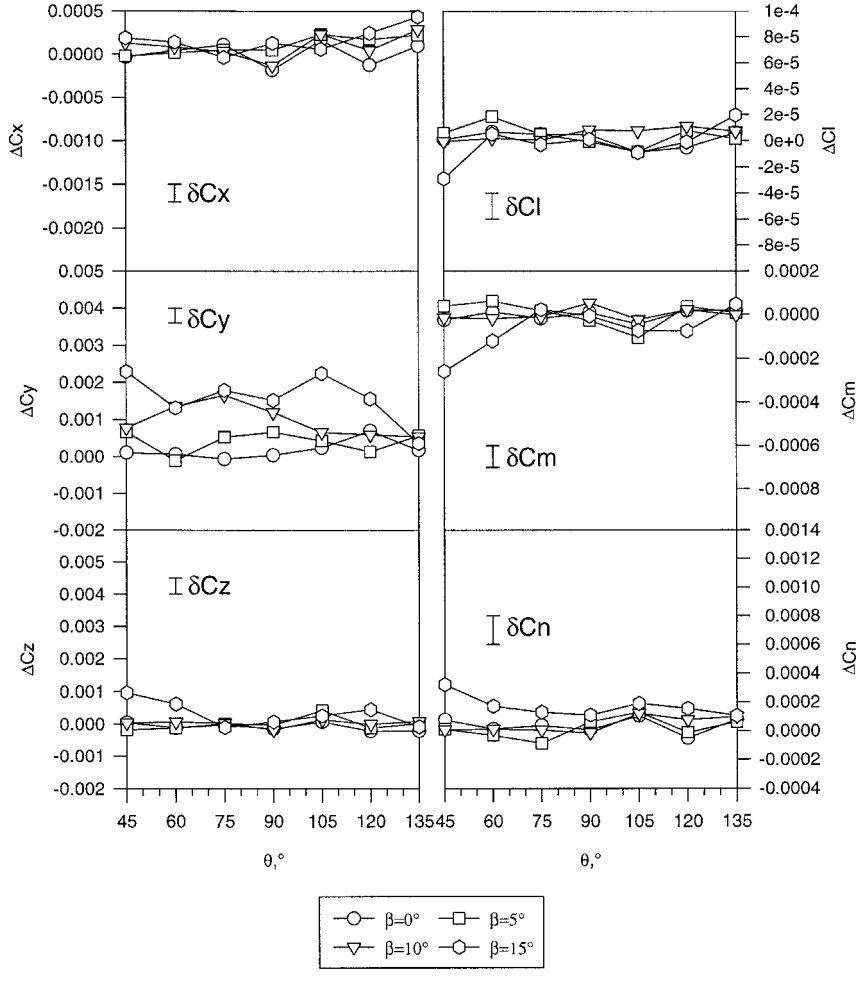

Fig. 14 Forces and moments vs skew angle θ for different *VR* for model 2 with jets. $Re = 4.6 \times 10^6$ and β = 15 deg.

Force and Moment Interpretation—Turning Performance

Traditionally, the dynamic performance analysis of airborne and waterborne vehicles has been limited to linear theory. It is evident that linear theory is limited because it does not account for unsteady separation effects. However, linear theory can provide first-order insights into the effects of configurational changes on the turning performance of a vehicle. A more detailed analysis of the effects of vortex generators on the turning performance of a submersible vehicle can be found in Ref. 16.

In linear theory it is the slope of force and moment curves with respect to flow parameters (like sideslip angle) that determines vehicular maneuvering performance.[18] Performance is expressed traditionally in terms of stability, and so an improvement in turning performance requires a decrease in stability. For the assumed configuration the vortex generators are both deployable and have variable orientation, but the plots in Fig. 10 show variations of forces and moments for fixed fin orientation. Therefore, in practice, at β = 0 deg the generators would not be deployed, and the forces and moments would be represented by the naked body data on the plots in Fig. 10. At 15-deg sideslip, it can be assumed that the generators would be optimally deployed, and so the forces and moments would be given by the data for the vehicle with fins. These two data points are then used for the present discussion to define the new force and moment slopes for the vehicle with deployable generators.

By examining Fig. 10 it can be seen that the vortex generators decrease both the $C_y - \beta$ and $C_n - \beta$ slopes significantly. Unfortunately, these two trends counteract each other from a stability standpoint.[17] The true effect of vortex generators on the turning performance of a submersible vehicle is dependent on the relative magnitude of these terms and the resultant effect on the yaw rate derivatives, which have not been measured. Therefore, from a linear standpoint, no definite turning performance effects can be predicted with these data. Further studies aimed specifically at turning performance evaluation, as opposed to fluid-dynamics-oriented research, must be pursued.

One idea that was not pursued was the concept of using vortex generators to augment separation; that is, one could orient the vortex generators to create vortices of like sign to the crossflow separation, presumably making separation occur earlier than in the naked vehicle case and drastically changing the forces and moments in the opposite direction (increasing side force and yaw moment). It is likely that by selectively augmenting the separation on one portion of the vehicle and countering separation on another part of the vehicle, one could control the forces and moments acting on the vehicle to guarantee a significant improvement in turning performance.

In future work consideration must be taken for the effect of the vortex generators on all forces and moments, particularly drag, and the resultant effect these forces and moments have on the vehicle's turning trajectory. The large increase in drag because of the deployment of the fins may have the largest effect on the turning performance. A large drag may result in an exorbitant amount of time to make the turn, or may result in lower exit velocity. On the other hand, the higher drag will result in less drift of the vehicle and may allow even tighter radius turns.

Conclusions

The turning performance of a submersible vehicle is adversely affected by the crossflow separation off the leeward side. Vortex generators offer a possible means of lessening that

crossflow separation and improving turning performance. Fins placed along the top and bottom centerlines from bow to stern dramatically reduce crossflow separation on a submersible vehicle in a sideslip. Oil-flow visualization shows that, with the addition of fins, the peripheral angular location of separation can be delayed by as much as 37 deg. Similar jet configurations at 30 deg inclination, velocity ratios up to 3.5, and various skew angles did not delay separation.

The fins tremendously alter the force and moment distribution. With the addition of the vortex-generating fins C_y was reduced by up to 50%, C_x was increased by up to 300%, and C_n was decreased up to 35%. In addition, C_z and C_m were increased by up to 300% and C_l was unaffected. Skew angles of 30 to 45 deg are most effective.

During tests in which the number of fins on the submersible vehicle was varied, it was found that the forward-mounted appendage plays a critical role in the effectiveness of a vortex-generator configuration. Because the flow separates off the forward-mounted appendage leading edge at $\beta = 15$ deg, the separation line immediately aft of this appendage is pinned to the appendage trailing edge regardless of the vortex generator system. Therefore, the vortex generators delay separation by different amounts on the top and bottom of the submersible vehicle, which induces the severe out-of-plane forces and moments. The same series of tests revealed that the rear fins are responsible for reductions in side force, while forward fins are responsible for reductions in yaw moment.

As a concept, the fins are definitely a viable means for flow control. Further reductions in separation could most likely be achieved by more carefully optimizing size, shape, distribution, and orientation of the vortex generator system. Also, it is proposed that the fins could be used to increase separation, having an opposite effect on the forces and moments. By selectively increasing or decreasing separation at different locations on the body, one can independently control side force and yaw moment, thus guaranteeing that a significant improvement in turning performance can be achieved. To make quantitative conclusions about turning performance, unsteady dynamic tests with transient flow effects must be performed. For the first time such tests are available with the new dynamic plunge-pitch-roll model mount (DyPPiR) at the Virginia Tech Stability Wind Tunnel.

The concept pursued in this study, while originally intended for marine applications, is equally well suited for any configuration where three-dimensional separation control is desirable. This includes using the fins as a control effector for very maneuverable missiles or controlling separation on the nose or fuselage of an aircraft.

Acknowledgments

This work was supported by the National Science Foundation through a Graduate Fellowship and the Defense Advanced Research Projects Agency (Gary W. Jones, Program Manager) through the Office of Naval Research Grant N00014-91-J-1732 (James A. Fein, Program Manager). We also thank S. Ha for performing the hot-wire measurements.

References

[1]Bushnell, D. M., and Donaldson, C. D., "Control of Submersible Vortex Flows," NASA TM-102693, June 1990.

[2]Pearcey, H. H., "Shock-Induced Separation and Its Prevention by Design and Boundary Layer Control," *Boundary Layer and Flow Control, Its Principal and Applications*, edited by G. V. Lachman, Vol. 2, Pergamon, Oxford, England, UK, 1961, pp. 1166–1344.

[3]Bragg, M. B., and Gregorek, G. M., "Experimental Study of Airfoil Performance with Vortex Generators," *Journal of Aircraft*, Vol. 24, No. 5, 1987, pp. 305–309.

[4]Chesnakas, C. J., and Simpson, R. L., "A Detailed Investigation of the 3-D Separation About a 6:1 Prolate Spheroid at Angle of Attack," AIAA Paper 96-0320, Jan. 1996.

[5]Poll, D. I. A., "On the Effects of Boundary Layer Transition on a Cylindrical Afterbody at Incidence in Low-Speed Flow," *Aeronautical Journal*, Vol. 89, No. 1037, 1985, pp. 315–327.

[6]Ahn, S., and Simpson, R. L., "Cross-Flow Separation on a Prolate Spheroid at Angles of Attack," AIAA Paper 92-0428, Jan. 1992.

[7]Compton, D. A., and Johnston, J. P., "Streamwise Vortex Production by Pitched and Skewed Jets in a Turbulent Boundary Layer," *AIAA Journal*, Vol. 30, No. 3, 1992, pp. 640–647.

[8]Morin, B. L., Simonich, J. C., Patrick, W. P., and Schlinker, R. H., "An Experimental Investigation of Surface Contouring and Vortex Generators for Wake-Mixing Enhancement and Separation Alleviation on Marine Vehicles," United Technologies Research Center, Rept. R91-958356, 1991.

[9]Morin, B. L., Patrick, W. P., and Schlinker, R. H., "A Parametric Study of Vortex Generator Jets for Three-Dimensional Separation Alleviation," United Technologies Research Center, Rept. R92-970141, Oct. 1992.

[10]Huffman, J. K., and Fox, C. J., "Subsonic Lateral/Directional Static Aerodynamic Characteristics of a General Research Fighter Configuration Employing a Jet Sheet Vortex Generator," NASA TM-74049, Jan. 1978.

[11]Malcolm, G. N., and Skow, A. M., "Enhanced Controllability Through Vortex Manipulation of a Fighter Aircraft at High Angle of Attack," AIAA Paper 86-2277, Aug. 1986.

[12]Ng, T. T., and Malcolm, G. N., "Aerodynamic Control Using Forebody Blowing and Suction," AIAA Paper 91-0619, Jan. 1991.

[13]Ziegler, H., and Wooler, P. T., "Aerodynamic Characteristics of a Jet Sheet Vortex Generator," NASA CR-158904, June 1978.

[14]Lin, J. C., Howard, F. G., Bushnell, D. M., and Selby, G. V., "Investigation of Several Passive and Active Methods for Turbulent Flow Separation Control," AIAA Paper 90-1276, June 1990.

[15]Johnston, J. P., and Nishi, M., "Vortex Jets—A Means for Flow Separation Control," *AIAA Journal*, Vol. 28, No. 6, 1990, pp. 989–994.

[16]Wetzel, T. G., Simpson, R. L., and Liapis, S., "The Effect of Vortex Generating Fins and Jets on Crossflow Separation on a Submarine in a Turning Maneuver," Virginia Polytechnic Inst. and State Univ./Aerospace and Ocean Engineering, Rept. VPI-AOE-195, DTIC, ADA2660470XSP, 1993.

[17]Ha, S., "An Experimental Study of Coherent Structure in a Turbulent 3-D Boundary Layer," Ph.D. Dissertation, Aerospace and Ocean Engineering Dept., Virginia Polytechnic Inst. and State Univ., Blacksburg, VA, 1993.

[18]Burcher, R., and Rydill, L., *Concepts in Submarine Design*, Cambridge Univ. Press, New York, 1994.

[19]Bertin, J. J., and Smith, M. L., *Aerodynamics for Engineers*, Prentice–Hall, Englewood Cliffs, NJ, 1989, pp. 282–289.